ELSEVIER

Chemical Engineering Journal 126 (2007) 119–130

Chemical Engineering Journal

www.elsevier.com/locate/cej

Preparation and characterization of Ce-Zr and Ce-Mn based oxides for *n*-hexane combustion: Application to catalytic membrane reactors

G. Picasso, M. Gutiérrez, M.P. Pina *, J. Herguido

Department of Chemical & Environmental Engineering, University of Zaragoza, 50009 Zaragoza, Spain

Received 13 July 2006; received in revised form 11 September 2006; accepted 12 September 2006

Abstract

Ce-Mn and Ce-Zr catalytic samples with different Ce/metal molar ratio have been prepared by coprecipitation followed by calcination at moderate temperatures (350–450 °C) and characterized by XRD, XPS, BET, TPR and SEM–EDX techniques. The preparation procedure of analogous catalytic membranes over γ-Al_2O_3 ceramic supports has been also studied in order to control loading, distribution and composition of the catalytic material inside the membrane thickness. To evaluate their catalytic performance, the combustion of *n*-hexane from air-diluted streams has been carried out in both a conventional fixed bed reactor and a flow-through catalytic membrane reactor operating in Knudsen diffusion regime. Surface area alone cannot account for the reaction performance achieved; however, the redox properties and oxygen mobility of the mixed oxides have been revealed as key parameters controlling the catalytic activity. Although Ce-Mn powdered catalysts appear more active in *n*-hexane combustion than their Ce-Zr counterparts; a strong deactivation phenomenon, more severe for Mn rich samples, is observed with time on stream in contrast with Ce-Mn based membranes showing catalytic stability under equivalent reaction conditions.

Keywords: Ce-Zr mixed oxides; Ce-Mn mixed oxides; Redox properties; Hexane combustion; Catalytic membrane reactors

1. Introduction

Volatile organic compounds are an important class of pollutants responsible of photochemical ozone in the ground level and other oxidants. They are found in urban and industrial areas due to the emissions of vehicles, industrial processes and human activities. The total removal of highly toxic volatile organic compounds (VOC's) without secondary pollutants requires the best achievable technology (BAT) in particular when their elimination has to be ensured at moderate temperatures for savings in energy costs [1]. During last years, catalytic combustion has acquired an increasing importance for VOCs abatement due to NO_x and other secondary atmospheric hazards [2] formation is substantially depressed.

The most common catalysts used to control VOC emissions can be classified in two main groups: noble metals and metal oxides. Most of catalytic systems used in VOC control incinerators are still based in supported noble metals such as Pt [3–5], Pd [6], Au [7,8]. Recently, metal oxide based catalysts such as Cr_2O_3, CuO [9,10] are increasingly applied in combustion systems in order to reduce costs associated to catalyst inventario. Among several metal oxides, particular attention is being paid to the application of CeO_2 based catalysts for environmental purposes due to the unusual redox behavior of ceria and its high oxygen storage/transport capacity (OSC) [11]. Incorporation of other oxides such as ZrO_2 into ceria lattice enhances redox properties providing high thermal stability [12]. The CeO_2-ZrO_2 mixed oxides are well known in TWC technology and have found some interesting applications as industrial catalysis [13]. A great part of the research efforts has been focused on catalyst preparation in order to obtain Ce-Zr mixed oxides with elevated surface area. Among the synthesis methods, the coprecipitation procedure from the corresponding salts has found recurrent application owing to the high oxygen storage capacity achieved by the final material [14–17]. Several papers dealing with Mn based catalysts have been published over the last 5 years. Mn confined in perovskite structures [18,19], supported on alumina-coated monoliths [20] or just employed as simple oxide MnO_x [21–23] have been well studied as VOC removal catalysts due to the redox properties of the system. Moreover, Ce-Mn catalysts have been investigated for the combustion of CO [24], *n*-butane [25] and for pollutants removal from

* Corresponding author. Tel.: +34 976 76115; fax: +34 976 762142.
E-mail address: mapina@unizar.es (M.P. Pina).

1385-8947/$ – see front matter © 2006 Elsevier B.V. All rights reserved.
doi:10.1016/j.cej.2006.09.005

aqueous streams by the catalytic wet air oxidation processes [26–30].

The *n*-hexane combustion at ppm level has already been used as model reaction to evaluate the catalytic performance of different catalytic systems [7,19,31]; however, to the best of our knowledge Ce-Mn or Ce-Zr mixed oxides have not been previously reported for VOCs removal from gaseous streams. In this work, an evaluation of the catalytic properties of Ce-Zr and Ce-Mn based oxides in powder form and also supported on ceramic membranes has been carried out. The preparation procedures and the catalyst composition have been investigated in order to establish the most favourable conditions for VOC removal for being used in the catalytic membrane reactor development. With the introduction of commercially available porous inorganic membranes, there has been a dramatic surge of interest in the field of inorganic membrane reactors for catalysis, driven by the enormous potential payoff of this technology [32]. The concept of a flow-through catalytic membrane reactor operating in Knudsen diffusion regime as an efficient gas–solid contactor has already been evaluated in our previous works [33–37] for VOCs abatement. In nearly all these cases, the direct impregnation of the porous support with salt solutions has been employed for the synthesis of porous infiltrated composite membranes. Some experimental parameters for membrane activation such as filtration period, deposition stage and reagent-support contact configuration have been carefully studied for single oxides (i.e. Fe_2O_3) [37] addressing to achieve a confinement of the catalyst inside the membrane top layer. The previous experimental results obtained with Pt/γ-Al_2O_3 [33–35] or metal oxides [36,37] based membranes indicate that the confinement of catalytic material inside the mesoporous layer of a γ-alumina membrane support, where the Knudsen diffusion is prevalent, allowed to minimize gas–solid bypass and consequently total conversion was achieved at lower temperatures. However, the incorporation of mixed oxides into the membrane involves additional issues related to different diffusion properties of metal precursors which could affect the Ce/metal distribution profiles along the membrane thickness. Moreover, a multi-step impregnation is not well adapted for precisely controlling the composition of the mixed oxide based membrane material. Therefore, a great part of the present work is devoted to analyze the different factors controlling the location of the catalytic material inside the porous support.

2. Experimental

The majority of bulk catalysts (see Table 1 for composition) have been synthesized by coprecipitation adding dropwise a concentrated NH_4OH solution (30 wt%, Panreac) to an aqueous solution of the appropriate composition containing $Ce(NO_3)_3{\cdot}6H_2O$, $ZrO(NO_3)_2{\cdot}xH_2O$, and $Mn(NO_3)_2{\cdot}xH_2O$ (all of them Aldrich, 99.99% pure). Additionally, pure single oxides CeO_2, ZrO_2 and Mn_xO_y have been prepared as reference supports using the same process. This experimental method denoted as A, has been the standard one, in contrast with procedure B for which the mixed oxide precursor was added to an excess (aproximately 100%) of ammonium hydroxide [14,28]. The "as prepared" B samples have been identified with suffix "b". After precipitation, the solids have been filtered, washed with deionized water until no pH change, dried at 100 °C for 24 h and then calcined in air. The aim of this work is devoted to prepare catalytic membranes highly active for VOCs combustion, therefore thermal treatments have been studied in detail to maintain elevated surface area. According to the literature, the standard calcination temperature used for manganese-cerium composite oxides is 350 °C for 3 h [28–30] whereas for Ce-Zr based oxides it has been demonstrated the solid oxide formation at 500 °C for 1 h [14,15]. In this work, a calcination procedure involving 350 °C for 3 h has been used for both catalytic systems; whereas, 450 °C for 3 h has also been studied for Ce-Zr samples (catalysts denoted with suffix "h").

Table 1
Characteristics of the bulk catalysts prepared in this work

Samples[a]	Precipitation method	Calcination conditions	S_{BET} (m^2/g)
CeO_2	A	350 °C, 3 h	51.0
$Ce_{0.78}Zr_{0.22}O_2$	A		40.9
$Ce_{0.78}Zr_{0.22}O_2$b	B		89.1
ZrO_2	A		39.1
CeO_2h	A	450 °C, 3 h	48.6
$Ce_{0.78}Zr_{0.22}O_2$h			35.3
ZrO_2h			29.7
Mn_xO_y	A	350 °C, 3 h	19.4
$Ce_{0.33}Mn_{0.67}O_2$	A		73.2
$Ce_{0.5}Mn_{0.5}O_2$	A		69.9
$Ce_{0.5}Mn_{0.5}O_2$b	B		87.1
$Ce_{0.67}Mn_{0.33}O_2$	A		65.9
$Ce_{0.78}Mn_{0.22}O_2$	A		65.5

[a] Formulation in accordance with the composition of the starting precursor solution.

The powder surface area after calcinations has been determined by BET measurements, using a Pulse Chemisorb 2700 Micromeritics. Prior to adsorption experiments samples are degassed overnight at 200 °C. X-ray diffractograms have been collected with a Rigaku/Max System using Cu Kα radiation (λ = 1.5418 Å) from 5 to 80° with a step size of 0.10° and a step time of 2.5 s. The data were compared to reference data from the International Centre for Diffraction Data for identification purposes. Data processing was accomplished using the Accelrys MS Modeling V 3.2 software package. Lattice parameters were calculated using Treor90 method as indexing program. Temperature programmed reduction experiments have been performed in a quartz reactor (6 mm internal diameter and 310 mm length) using a mixture of 6% H_2 in N_2 flowing at 100 ml/min and heating the samples (ranging from 75 to 220 mg) from 25 to 650 °C following a rate of 5 °C/min linear temperature rise.

The catalytic combustion of *n*-hexane was performed in a 9-mm internal diameter tubular quartz reactor inside an electrical furnace operating at atmospheric pressure. The experimental conditions (gas velocity and particle diameter) were adjusted to minimize mass-transport resistances. The reaction temperature was monitored by a thermocouple inserted in the

Table 2
Main properties of the catalytic Ce-Zr and Ce-Mn based membranes developed in this work

Samples	Composition[a]	Calcination	Weight gain (%)[b]	Knudsen Contribution (%)	N_2 permeation flux (mol/m^2 s Pa)
MB-0	Blank	–	–	92.8	6.24×10^{-6}
MB/C	CeO_2		0.83	–	–
MB/Z	ZrO_2	350 °C, 3 h	0.40	–	–
MB/M	Mn_xO_y		0.46	–	–
MB/CZ-1			0.41	96.8	3.03×10^{-6}
MB/CZ-2		350 °C, 3 h	0.30	93.5	3.15×10^{-6}
MB/CZ-3	Ce/Zr = 1		0.55	92.7	3.04×10^{-6}
MB/CZ-4		350 °C, 9 h	0.39	94.9	3.07×10^{-6}
MB/CZ-5		450 °C, 3 h	1.14	92.1	2.54×10^{-6}
MB/CM-1		350 °C, 3 h	0.33	96.3	1.97×10^{-6}
MB/CM-2	Ce/Mn = 1		0.34	95.1	1.42×10^{-6}
MB/CM-3[c]		350 °C, 9 h	0.34	–	–
MB/CM-4[c]		350 °C, 12 h	0.34	–	–
MB/C[d]	CeO_2		0.54	–	–
MB/Z[d]	ZrO_2		0.52	–	–
MB/M[d]	Mn_xO_y	350 °C, 3 h	0.18	–	–
MB/CZ[d]	Ce/Zr = 1		0.67	–	–
MB/CM[d]	Ce/Mn = 1		0.34	–	–

[a] Atomic ratio of metals in the precursor solution used for membrane impregnation.
[b] Calculated per gram of porous membrane.
[c] Prepared from thermal treatments of MB/CM-2.
[d] Intermediate drying period of 30 min (instead of 24 h).

center of the catalyst bed in which 100 mg of catalyst diluted in 200 mg of glass dust, to avoid hot spots formation, was introduced and fixed over a trap. An analysis section, comprising an on-line gas chromatograph (FID detector) and a methanation unit to monitor continuously CO and CO_2, were used to check carbon balances (±5%). $T_{50\%}$ and $T_{95\%}$ are defined as temperatures for 50 and 95% conversion levels, respectively. A more detailed description of experimental set up has been made in previous works [33–37]. The *n*-hexane combustion experiments were performed using 80 h^{-1} as weight hourly space velocity (WHSV) defined as the ratio mass of catalyst total mass gas flow and 2000 ppmV as initial VOC concentration.

Catalytic membranes were prepared from 90 mm long, 10 mm o.d. asymmetric ceramic tubes (Inocermic) with 5 nm pores in the γ-Al_2O_3 thin layer (5 μm of thickness). The ends of the ceramic supports were sealed with a glazing compound to allow for mounting in the experimental setup for permeation and reaction experiments. The total length of the porous part available for catalyst deposition ranged was around 55 mm. The catalytic material deposited over the membranes was obtained by the "precipitation method" already described in literature [37] for Fe_2O_3 based catalytic membranes. It basically consisted on the support impregnation with the precursor solution fed to the internal side, a subsequent washing with deionised water from the outside to the inside followed by an intermediate drying at room temperature and a final NH_4OH impregnation from the inner surface. After drying at 25 °C for 24 h, the membranes were calcined under similar conditions to those used for powder catalysts. However, for the mixed oxide membranes developed in this work, the activation process was carefully explored in order to analyze the influence of impregnation time, concentration of precursor solution, intermediate drying period and reagent–contact configuration on the catalyst loading and distribution inside the membrane. For such purpose, shorter membranes (approximately 30 mm in length) were prepared for being further analyzed by SEM–EDX in order to obtain metal distribution profiles (detection limit around 1 at.%) and establish the most adequate conditions in terms of catalyst confinement within the top layer. Moreover, X-ray photoelectron spectroscopy (XPS) analysis were also carried out to characterize the atomic surface composition of the membranes and the chemical environment of the metals involved for comparison purposes with their powder counterparts. These analyses were performed with an Axis Ultra DLD (Kratos Tech.). The spectra were excited by the monochromatized Al Kα source (1486.6 eV) run at 15 kV and 10 mA. For the individual peak regions, a pass energy of 20 eV was used whereas the survey spectrum was measured at 120 eV. Analyses of the peaks were performed with the software provided by the manufacturer, using a weighted sum of Lorentzian and Gaussian components curves after background subtraction.

Table 2 compiles the main properties of the catalytic membranes tested for *n*-hexane combustion including the percentage of Knudsen contribution to total N_2 permeation flux evaluated at 1 bar as average pressure in accordance with the expression suggested by Keizer et al. [38]. Reaction experiments were carried out in a flow-through membrane reactor operating in Knudsen diffusion regime [33–37] using the experimental conditions established for powder catalysts.

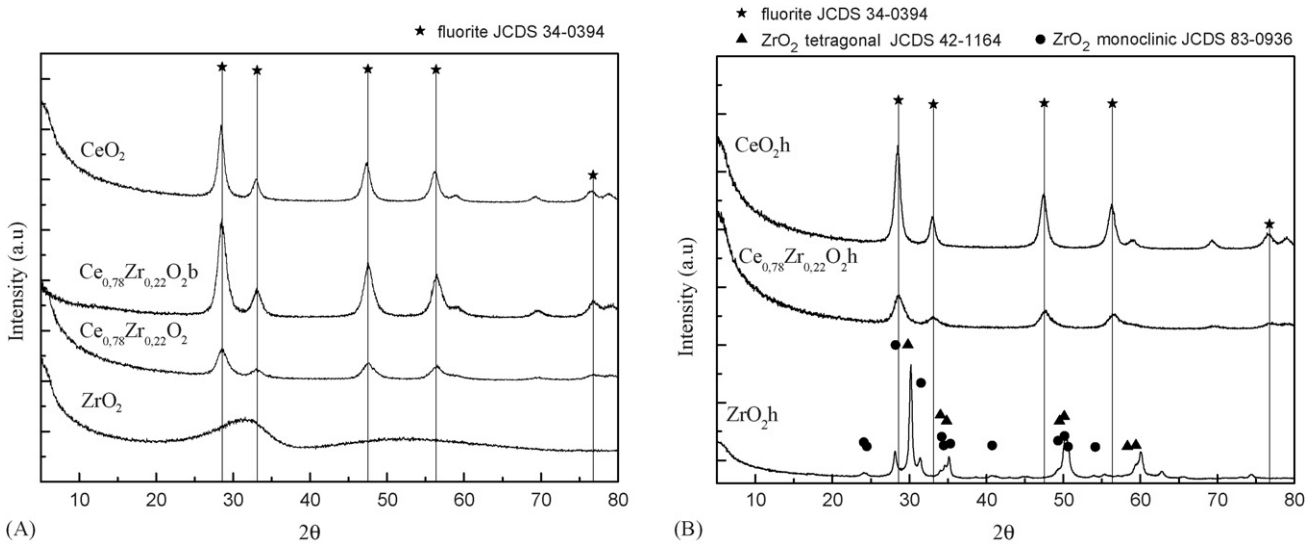

Fig. 1. XRD spectra of: (A) Ce-Zr bulk catalysts calcined at 350 °C and (B) Ce-Zr bulk catalysts calcined at 450 °C.

3. Results and discussion

3.1. Bulk catalyst characterization

The XRD spectra of the bulk catalysts listed in Table 1 are shown in Fig. 1A and B for Ce-Zr, and Fig. 2 for Ce-Mn samples, respectively. The crystallographic patterns of pure singles oxides have also been included as reference supports (i.e. CeO_2 (JCDS 34-0394), ZrO_2 with tetragonal (JCDS 42-1164) and monoclinic (JCDS 83-0936) symmetry and Mn_xO_y oxides (JCDS 24-0735, JCDS 33-0900, JCDS 80-0382)). As it was already mentioned, in addition to the standard calcination procedure (350 °C, 3 h), the Ce-Zr samples have also been calcined at 450 °C for 3 h (see Fig. 1B) in order to develop a crystalline structure for pure zirconium oxide at the expense of a catalyst surface area loss (up to 24% for ZrO_2 samples). A mixture of monoclinic and tetragonal structures crystalline phases is obtained for ZrO_2h catalyst, in accordance with the published literature [16].

Neither phase due to pure ceria nor pure zirconia have been observed in the XRD spectra of the mixed samples. Ceria as well as the Ce/Zr samples, are characterized by a face centered cubic cell typical of the fluorite structure; however, a decrease of the unit cell parameter "a" is observed by the introduction of zirconium into ceria lattice (5.413 for CeO_2h versus 5.378 for $Ce_{0.78}Zr_{0.22}O_2$h). Such a decrease was already observed by other authors [39,40], and it was assigned to the lower ionic radius of Zr^{+4} (0.84 Å) compared to that of Ce^{+4} (0.97 Å).

It is worthwhile to remark that $Ce_{0.78}Zr_{0.22}O_2$b sample develops the higher surface area of the Ce-Zr system (89.1 m^2/g), signifying that "B" procedure leds to high surface area materials. A similar behaviour is shown by $Ce_{0.5}Mn_{0.5}O_2$ samples for which a 25% of surface area increase is attained (87.1 m^2/g versus 69.9 m^2/g). Moreover, the BET surface area for Ce-Zr composites do not overcome the values achieved for pure ceria whatever the calcination procedure used.

Fig. 2 shows the powder XRD patterns of the Ce-Mn catalyst samples, including single oxides. For pure manganese oxide sample, i.e. Mn_xO_y, typical diffraction peaks for MnO_2 (JCDS 24-0735), Mn_2O_3 (JCDS 33-0900), and Mn_3O_4 (JCDS 80-0382) were identified. This means that in cerium-free sample, Mn occurs in +2, +3 and +4 oxidation states. For mixed oxide samples, no manganese oxide phases were detected by XRD, and the dominant diffraction peaks are the characteristic of cerianite (JCDS 34-0394). This may be due to the formation of Ce-Mn solid solutions with fluorite structure. However, a systematic peak width broadening was observed with increasing manganese content, a similar trend already observed by other authors [30], indicating the occurrence of more defective cerianite lattice, lower degree of crystallinity and smaller particle size; which indeed hindered the data processing for lattice parameter estimation. These results are in accordance with the BET surface area increase with increasing contents of manganese (see Table 1), i.e. from 65.5 m^2/g for $Ce_{0.78}Mn_{0.22}O_2$ to 73.2 m^2/g for

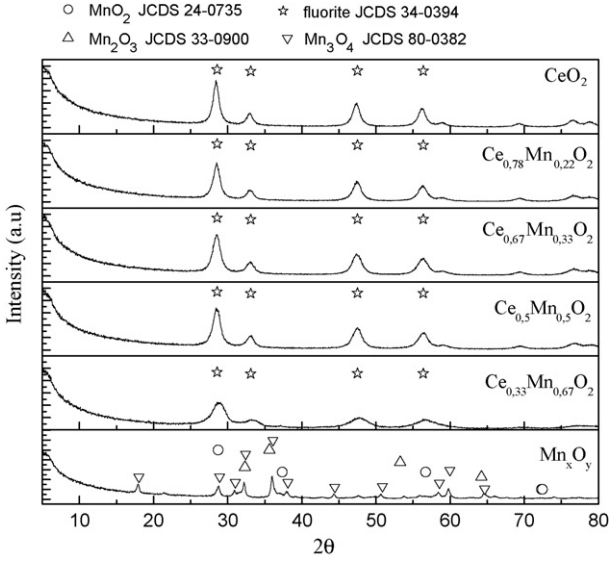

Fig. 2. XRD spectra of Ce-Mn bulk catalysts.

$Ce_{0.33}Mn_{0.67}O_2$. Unlike Ce-Zr series, the surface area of all the composite oxide samples outweighed that predicted for mere mechanical mixtures of pure Mn_xO_y and CeO_2 single oxides with 19.4 and 51 m^2/g, respectively. This suggests a strong intimate interaction between manganese and cerium oxides.

TPR experiments have been carried out over Ce-Mn samples in order to study the influence of cerium content on the redox properties and to ensure the formation of Mn-O-Ce composites at the calcination temperatures used in this work (i.e. 350 °C for 3 h). It is well demonstrated that the interaction of Mn and Ce in composite oxides heavily modifies the redox activity of manganese, increasing lattice oxygen lability [13,24,26] with the promotion of the oxidation activity. On the other hand, the introduction of zirconia into ceria leads to the formation of solid solutions showing an improvement in the oxygen storage capacity as well as the oxygen mobility over pure ceria [14,39,40]; however,

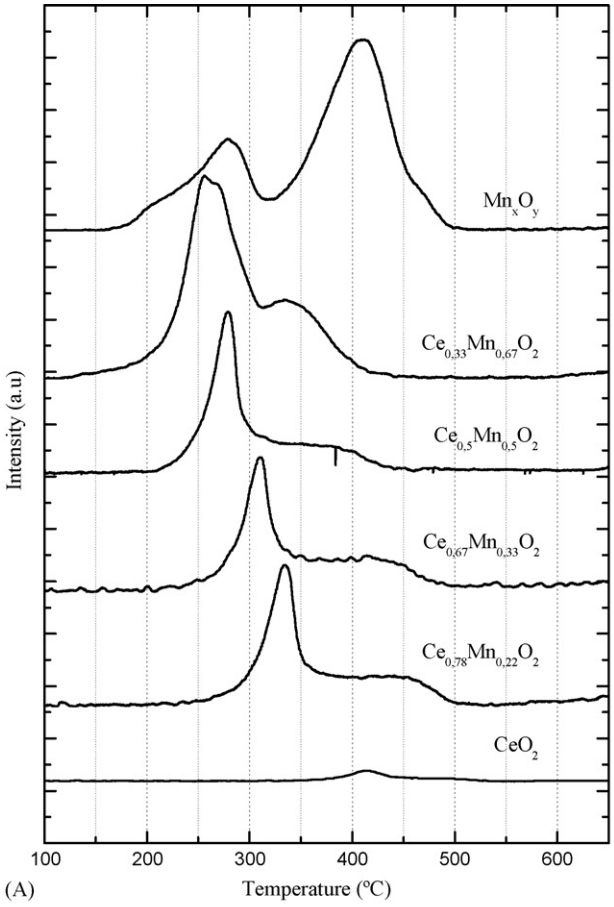

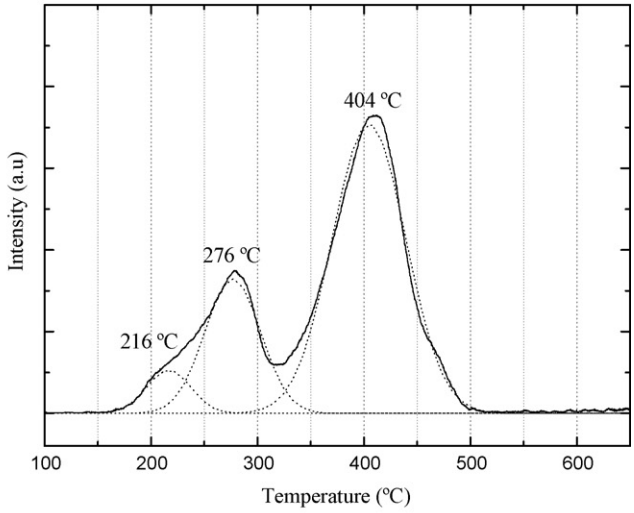

Reduction Step	H_2 consumption (peak area %)
$MnO_2 \rightarrow \alpha$-Mn_2O_3	6.2%
α-$Mn_2O_3 \rightarrow Mn_3O_4$	24.7%
$Mn_3O_4 \rightarrow MnO$	69.1%

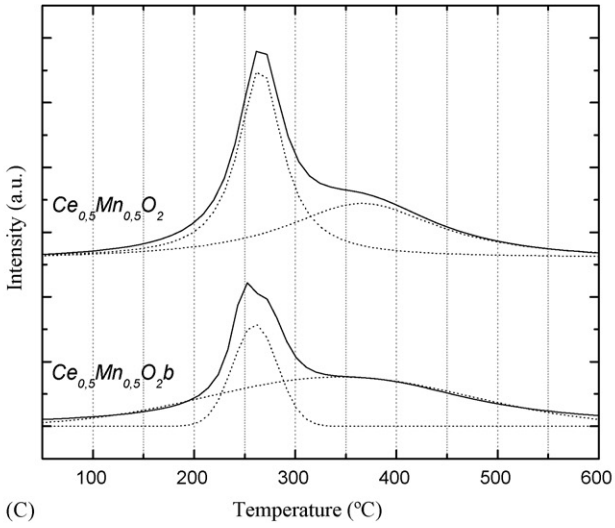

Fig. 3. (A) TPR profiles for Ce-Mn bulk catalysts. (B) TPR deconvolution analysis for Mn_xO_y sample. (C) TPR profiles for $Ce_{0.5}Mn_{0.5}O_2$ samples.

these solids have not been analyzed by TPR since their H_2 consumption peaks are centred at temperatures quite high enough to be revealed under *n*-hexane combustion reaction conditions.

The TPR patterns of the manganese-based catalysts, including pure oxides samples, are presented in Fig. 3A. It is important to remark in order to avoid misunderstandings that redox properties of Mn-O-Ce composites for Mn-rich samples clearly differ from Ce-rich catalysts [30]. A more detailed picture of the pure manganese oxide TPR profile is shown in Fig. 3.B. Three reduction peaks positioned at 216, 276 and 404 °C are observed, in accordance with the results of Gil et al. [41] for manganese oxide treated at 400 °C. These peaks are consistent with the following successive reduction steps: $MnO_2 \rightarrow \alpha$-$Mn_2O_3 \rightarrow Mn_3O_4 \rightarrow MnO$. The relative hydrogen consumptions of each reduction step, expressed as % peak area, are indicated in Fig. 3B. According to the literature, bulk manganese oxides can exhibit a variety of crystalline phases, depending mainly on the applied temperature and the atmosphere of calcinations. At low temperatures, manganese (IV) oxides are formed in a variety of structural forms. Among these, the most stable structure is β-MnO_2; however, the estimated contribution for the as prepared Mn_xO_y sample is scarcely about 6%. This can be attributed to the fact that thermodynamics does not adequately describe the chemistry of the manganese-oxygen system, especially at low temperatures, where the formation of manganese oxides of higher oxidation states is more kinetically than thermodynamically controlled [41].

The TPR analysis for Ce-Mn composites prepared in this work supports the formation of mixed oxide structures already demonstrated by the XRD results. The peak corresponding to the lower reduction temperature of pure manganese oxide is not clearly well defined, suggesting stronger interaction between the two oxide components. The reduction profiles are featured by two main peaks positioned at 260–330 °C and 320–380 °C, respectively; that systematically shift to higher reduction temperatures with increasing Ce content up to obtain the pure ceria profile which one reduction peak at 415 °C attributed to easily reducible surface Ce^{+4} species. Moreover, the area ratio of first to second peak also decreased with increasing cerium content, revealing that less manganese oxide species were in higher oxidation states.

The TPR profiles of $Ce_{0.5}Mn_{0.5}O_2$ samples prepared using different protocols, are compared in Fig. 3C. The area ratio of first to second peak also decreased around twice when procedure B is employed (from 0.66 to 0.35), indicating that more manganese oxide species were in higher oxidation states for the standard A procedure.

The oxidation states of surface species were characterized by XPS analysis. Fig. 4A shows the Mn 2p XPS spectra in the $Ce_{0.5}Mn_{0.5}O_2$ formulation compared to pure Mn_xO_y. The BE shifts towards higher values observed for mixed samples are indicating an interaction between manganese and cerium oxides [42]. However, the Mn $2p_{3/2}$ peaks are rather broad and the BE shifts are not resolved well enough to quantify the relative contribution of different manganese oxides. The energy positions of the spectral components in Ce $3d_{5/2}$ and Ce $3d_{3/2}$ for $Ce_{0.5}Mn_{0.5}O_2$ (not shown here) were found to be similar to those recorded from CeO_2 sample suggesting that the presence of manganese oxides does not alter the chemical environments of cerium in accordance with the published literature [43]. According to the semi-qualitative evaluation of the relative amount of cerium present as Ce^{+4} carried out in this work (calculated from the area of Ce $3d_{5/2}$ and Ce $3d_{3/2}$ peaks, respectively), the surface Ce^{+4}/Ce^{+3} atomic ratio is approximately the same for $Ce_{0.5}Mn_{0.5}O_2$ and CeO_2 samples (i.e. 1.36 and 1.46, respectively). Moreover, the surface XPS value of Ce/Mn ratio (calculated from the area of the Ce 3d and Mn 2p core levels) is larger than those in the bulk (i.e. 2.6 versus 1.0), indicating that the surface of the solid is enriched in Ce to some extent. For comparison purposes, Fig. 4A also shows the Mn 2p spectrum for the surface species dispersed over the Ce-Mn based membrane top layer. A similar behaviour to the bulk sample has been observed for the supported catalyst. On the other hand, the Ce 3d core level for MB/CM* sample is not resolved well enough (2% atomic concentration) to clearly distinguish the Ce(III) and Ce(IV) oxidation states.

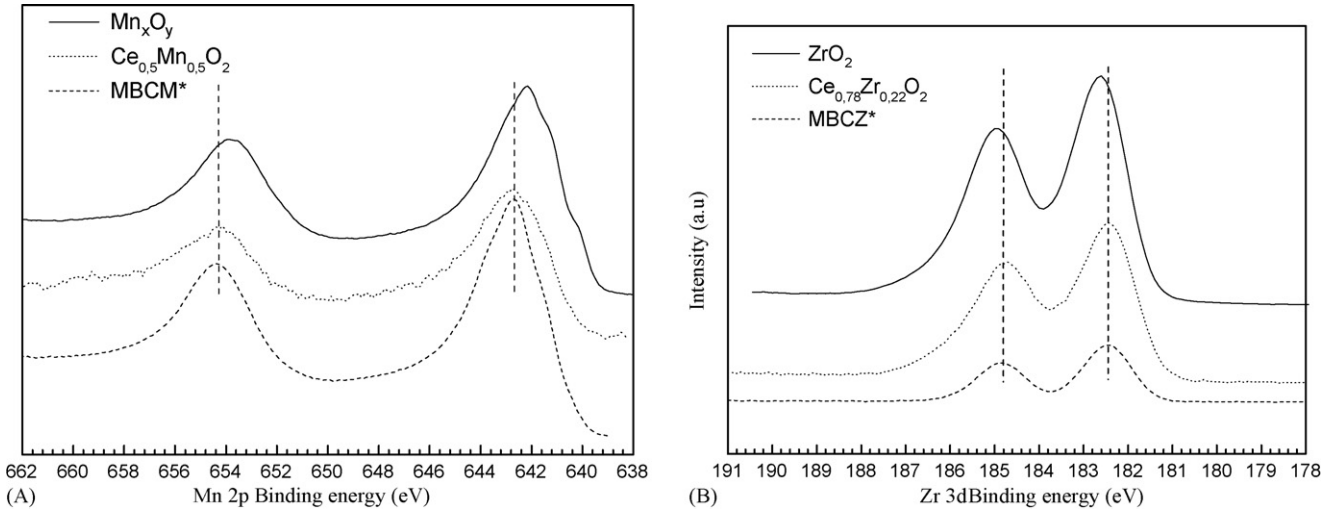

Fig. 4. (A) XPS spectrum of Mn 2p for different samples. (B) XPS spectrum of Zr 3d for different samples.

Fig. 4B shows the XPS spectra of Zr 3d in the $Ce_{0.78}Zr_{0.22}O_2$ sample compared to pure zirconia sample. The Zr 3d core level of ZrO_2 solid may be decomposed into two Gaussians corresponding to the $3d_{5/2}$ (182.6 eV) and $3d_{3/2}$ (185 eV) spectral components which remain nearly constant with Ce addition (182.4 and 184.8 eV). Similarly to Ce-Mn system, the energy positions of the spectral components in Ce $3d_{5/2}$ and Ce $3d_{3/2}$ for $Ce_{0.78}Zr_{0.22}O_2$ were found to be similar to those recorded from pure CeO_2 sample suggesting that the insertion of zirconium does not alter the chemical environments of cerium. The surface Ce^{+4}/Ce^{+3} atomic ratio is approximately the same for both (1.57 for $Ce_{0.78}Zr_{0.22}O_2$ versus 1.36 for CeO_2). When bulk and supported Ce-Zr based oxides are compared, no significant differences in the metal chemical environments arise. In addition, the surface XPS value of Ce/Zr ratio (calculated from the areas of the Ce 3d and Zr 3d core levels) for $Ce_{0.78}Zr_{0.22}O_2$ is slightly larger than those in the bulk (i.e. 4.2 versus 3.5) indicating that the surface of the solid is enriched in Ce to some extent. However, this effect is more pronounced for the MBCZ* sample which exhibits a Ce-Zr surface atomic ratio of 4.8.

3.2. Catalytic membrane physico-chemical characterization

As it was already mentioned, the preparation of mixed oxide membranes was carefully explored in order to analyze the influence of concentration of precursor solution, intermediate drying period and reagent–contact configuration on the loading, distribution and composition of the catalyst which is really achieved within the mesoporous top layer, trying to establish a correlation with the reaction performance accomplished in *n*-hexane combustion. From our previous experience with α-hematite based membranes [37], we have employed 3 min as standard impregnation time for mixed oxides based membranes. Among the different parameters studied, the intermediate drying step between impregnation and precipitation revealed as crucial for confinement purposes as it can be observed in Fig. 5 where the SEM–EDX distribution profile for a pure ceria catalytic membrane is shown.

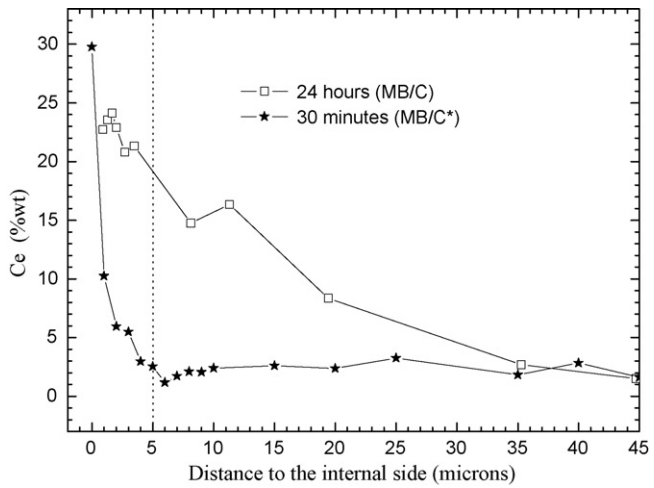

Fig. 5. Ce distribution profile as a function of the intermediate drying period.

All the Ce-Mn, Ce-Zr catalytic membranes tested in *n*-hexane combustion have been prepared by impregnation of a mixed nitrate solution (0.25 M in each metal) during 3 min. The incorporation of catalytic material makes the permeation values to decrease due to reduction of pore mean size. The blank membrane (MB-0) has a Knudsen contribution (92.8%) rather similar to those obtained for catalytic membranes (94.5% in average), indicating that the asymmetric structure of the starting alumina membranes is preserved in spite of the applied thermal treatments, reaction tests and mechanical manipulation. Therefore, we have developed a preparation method for Ce-based mixed oxide membranes which will allow us to validate the starting hypothesis for catalytic membrane reactor application, i.e. forced permeation flux under the Knudsen regime would give a considerably higher efficiency in the combustion of *n*-hexane from diluted streams. Under the experimental conditions tested in this work, the pressure drop across the catalytic membranes is twice the observed for the catalytic fixed bed reactor operation.

It was considered remarkable to study the influence of the mixed oxide precursor concentration on the catalyst distribution over the membrane thin layer, and some preliminary results are here anticipated. It should be remarked, however, that understanding the solution chemistry of cerium is not a simple task. Cerium ions may undergo complexation and hydrolysis depending on the ion concentration and pH, among others. Such solution parameters are rarely strictly the same when preparing CeO_2-ZrO_2 and CeO_2-MnO_2 based membranes.

In Fig. 6A, C and B, D the SEM–EDX analysis for Ce-Mn and Ce-Zr systems, respectively, prepared by impregnation during 3 min with the corresponding mixed nitrate are presented. The distribution profile exhibited by the pure oxide membranes prepared using identical conditions are also plotted as reference samples.

In general, the Ce percentage is higher in the mesoporous layer, and increases with the concentration of the mixed starting precursor for both catalytic systems. However, this effect is accompanied by a minor confinement in the Ce-Zr system for which a 12 wt% of Ce is detected up to 40 μm of distance to the internal side when 1.25 M in Ce^{+3} is used. In general, Ce loadings in the top layer are always higher for Ce-Mn membranes, and overcome those obtained for the pure ceria membrane. The Mn profile is similar to the one exhibited by Ce, i.e. a preferential location in the top layer affected by the precursor concentration (see Fig. 6C).

The Ce-metal atomic ratio distribution in the thin layer can be considered, as a first approach, indicative of the chemical composition of the catalyst material responsible of the *n*-hexane removal. In Fig. 7A, the Ce-Mn atomic ratio profiles as a function of precursor concentration have been compiled. A Ce enrichement in the mesoporous layer can be observed, in a more noticeable way (1.8 in average versus 1.5) for the sample prepared using a concentrated solution ($[Me^{n+}] = 1.25$ M) which indeed exhibits an excellent catalyst confinement and a total catalyst gain weight approximately seven times higher compared to the sample prepared using $[Me^{n+}] = 0.25$ M (28 mg/g versus 4 mg/g). In order to reduce Ce loadings pursuing an equimolar ratio within the top layer (the most active composition for

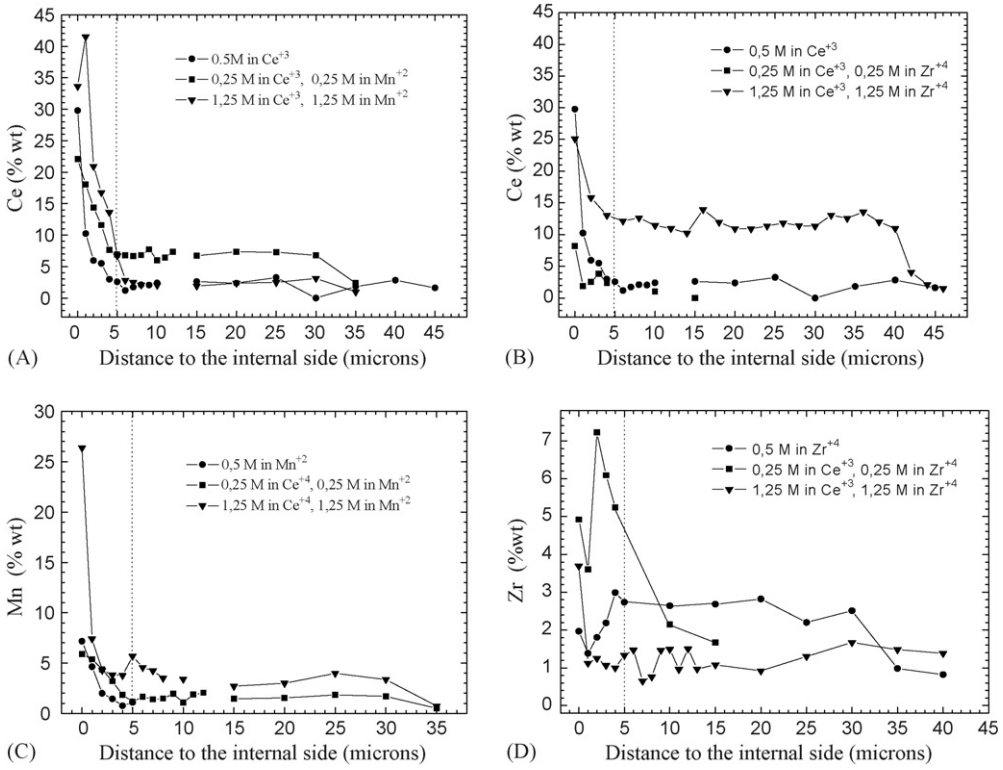

Fig. 6. (A) Ce distribution profile (wt%) as a function of concentration in the precursor solution for Ce-Mn catalytic membranes. (B) Ce distribution profile (wt%) as a function of concentration in the precursor solution for Ce-Zr catalytic membranes. (C) Mn distribution profile (wt%) as a function of concentration in the precursor solution for Ce-Mn catalytic membranes. (D) Zr distribution profile (wt%) as a function of concentration in the precursor solution for Ce-Zr catalytic membranes.

n-hexane combustion as is shown in Section 3.3), some samples were prepared using a Ce^{+3} concentration in the starting precursor five times lower than Mn^{+2}. However, far to improve the catalyst distribution, the Ce% atomic values measured were below the detection limit resulting in a 0.35 Ce-Mn atomic ratio as average value inside the mesoporous layer.

The influence of impregnation mode of the starting precursors, i.e. simultaneously or sequentially was also studied (not shown here) but no improvements were attained in terms of catalyst composition. Additionally, some samples were previously immersed in deionized water and externally wrapped with Teflon to reduce the precursor diffusion rate through the internal thin layer for confinement purposes. In such way, the metal loadings obtained were extremely low (i.e. below the detection limit) for being considered.

Taking into account the SEM–EDX analysis for Ce-Mn system, the most favorable preparation procedure will consist on: (i) a simultaneous impregnation with a mixed oxide precursor 1.25 M in each metal during 3 min, (ii) a posterior washing and drying at room temperature for 30 min, (iii) a subsequent impregnation with NH_4OH and (iv) a final calcination at 350 °C for 3 h. This protocole results in a 2.8% weight gain of catalytic material (expressed per gram of porous membrane) preferentially located in the mesoporous layer with a Ce-Mn atomic ratio circa 1.8.

On the other hand, Zr distribution profiles do not follow the expected behaviour with precursor concentration (see Fig. 6D);

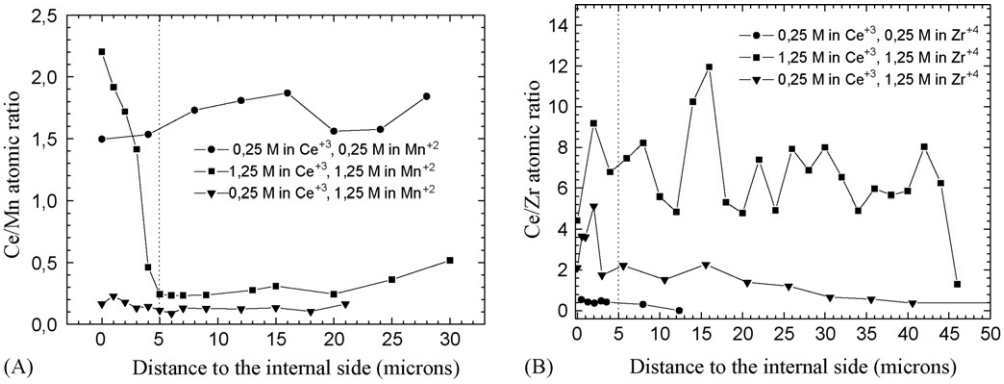

Fig. 7. (A) Ce-Mn atomic ratio profile as a function of starting precursor concentration for Ce-Mn catalytic membranes. (B) Ce-Zr atomic ratio profile as a function of starting precursor concentration for Ce-Zr catalytic membranes.

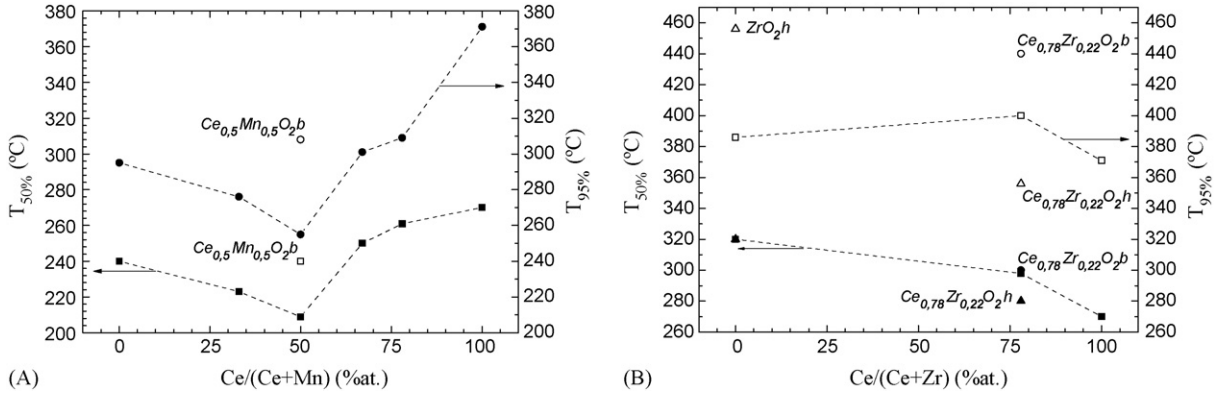

Fig. 8. (A) $T_{50\%}$ and $T_{95\%}$ for *n*-hexane combustion over Ce-Mn based catalysts. (B) $T_{50\%}$ and $T_{95\%}$ for *n*-hexane combustion over Ce-Zr based catalysts.

although the total catalyst gain weight is approximately five times higher for the sample prepared using $[Me^{n+}] = 1.25$ M, probably due to the wide Ce profile (see Fig. 6B). Moreover the Zr (at.%) values detected are the lowest in comparison with its counterparts; and always below the detection limit inside the membrane thickness with the exception of sample prepared using $[Me^{n+}] = 0.25$ M.

In order to improve catalyst location and loadings, some samples were prepared using a Ce^{+3} concentration (0.25 M) in the starting precursor five times lower than Zr^{+4} (1.25 M). As a result, the Ce confinement was greatly improved compared with sample prepared using $[Me^{n+}] = 1.25$ M. However, Zr loadings inside the membrane thickness remained below the detection limit, although the total catalyst gain weight was approximately seven times higher compared to the sample prepared using $[Me^{n+}] = 0.25$ M (22 mg/g versus 3 mg/g). In contrast with Ce-Mn system, an optimal procedure for Ce-Zr based membranes has not been already established. However, from the preliminary results here explained, the most favorable preparation procedure consists on: (i) a simultaneous impregnation with a mixed oxide precursor 0.25 M in Ce^{+3} and 1.25 M in Zr^{+4} during 3 min, (ii) a posterior washing and drying at room temperature for 30 min, (iii) a subsequent impregnation with NH_4OH and (iv) a final calcination at 350 °C for 3 h. This protocole results in a 2.2% weight gain of catalytic material (expressed per gram of porous membrane) with a Ce-Zr atomic ratio circa 2.1 on the external surface (see Fig. 7B).

3.3. Catalytic activity of bulk catalysts in n-hexane combustion

The catalytic performance of bulk catalysts prepared for this work has been evaluated using 80 h^{-1} as weight hourly space velocity (WHSV) and 2000 ppmV as initial VOC loading as reference conditions. However, reaction experiments carried out over pure CeO_2 catalyst at different initial *n*-C_6 concentrations (from 500 to 2000 ppmV) keeping constant the weight hourly space velocity, confirmed that the combustion of *n*-hexane is a pseudo-first order reaction referred to alcane concentration. A quite different picture from that observed in the combustion of MEK over the same catalyst in which the kinetic order was estimated lower than 1 related to oxygenate [44].

The temperatures required for 50 and 95% of *n*-hexane conversion are plotted as a function of Ce content (at.%) in Fig. 8A and B for Ce-Mn and Ce-Zr based catalytic systems, respectively. In Ce-Mn series a minimum is observed for sample $Ce_{0.5}Mn_{0.5}O_2$, which exhibits the lowest temperatures (i.e. $T_{50\%} = 208$ °C; $T_{95\%} = 255$ °C) for *n*-hexane combustion at reference conditions. Indeed, the equimolar sample showed the best behaviour considering BET surface area, crystallinity degree and redox properties (see Section 3.1). The BET surface area is not only the responsible of the catalytic performance. This fact is clearly demonstrated for sample $Ce_{0.5}Mn_{0.5}O_2$b which exhibit the higher surface area but the lower manganese oxide species content in higher oxidation states; leading to higher reaction temperatures (i.e. $T_{50\%} = 240$ °C; $T_{95\%} = 308$ °C).

From Fig. 8A, it seems that pure manganese oxides could be more active that some mixed oxide formulations; however, a serious deactivation effect with time on stream is observed (see Fig. 9). Some long-term analyses have been carried out to test the catalytic stability of the as prepared samples. In these experiments, firstly the *n*-hexane light-off curve at reference conditions is obtained; and after that, the catalyst temperature is kept constant at $T_{50\%}$ level to monitor continuously the VOC conversion. Fig. 10 shows the evolution of *n*-hexane conversion related to the

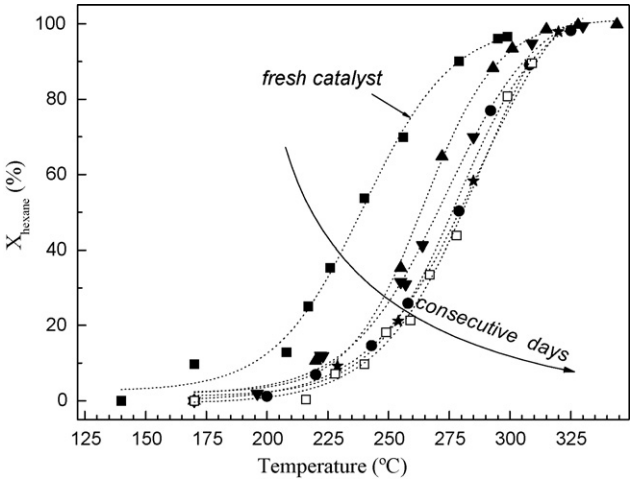

Fig. 9. Evolution of light-off curves for Mn_xO_y sample with time on stream. Reaction parameters: reference conditions.

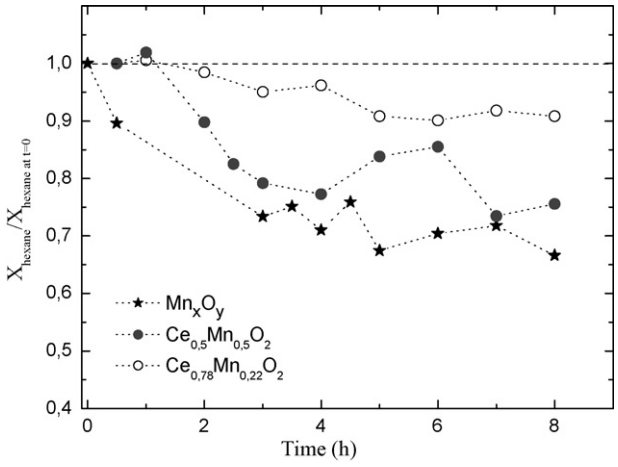

Fig. 10. Evolution of hexane conversion (related to the conversion obtained in the preliminary test) for some Ce-Mn powdered catalysts. Reaction parameters: $T^a = T_{50\%}$ for each sample and reference conditions.

conversion obtained in the preliminary light-off curve for different solids. As it can be observed, the higher Mn content, the more severe deactivation occurs. Additional experiments confirmed that such deactivation was due to the depletion of BET specific surface area (i.e 19.4 m^2/g for fresh Mn_xO_y to 10.3 m^2/g for "used" sample) which could be related with catalyst sintering at operation temperatures higher than 350 °C and/or formation of carbonaceous deposits over the active sites as a consequence of incomplete combustion of alcane. On the other hand, Ce-Zr based samples showed catalytic stability under equivalent reaction conditions.

All the Ce-Mn mixed solids present light-off temperatures lower than CeO_2; conversely, it is worthwhile to emphasize that pure ceria is the unique sample that exhibit total selectivity towards complete combustion products whatever the conversion level. Excepting ceria, the as prepared catalysts show a maximum yield to CO at $T_{50\%}$; in particular, the CO selectivities reported at light-off temperature have been less than 4 and 10% for Ce-Mn and Ce-Zr series, respectively.

In general, Ce-Mn powdered catalysts are also intrinsically more active in the combustion of *n*-hexane than Ce-Zr counterparts, probably due to the redox properties of the manganese mixed oxides (see Section 3.1). Among the Ce-Zr samples calcined at 350 °C, $Ce_{0.78}Zr_{0.22}O_2$b sample presents less oxidation activity that $Ce_{0.78}Zr_{0.22}O_2$ in spite of the specific surface area properties, similarly to $Ce_{0.5}Mn_{0.5}O_2$ b sample.

Considering Ce-Zr series on the whole, the $Ce_{0.78}Zr_{0.22}O_2$h sample (calcined at 450 °C for 3 h) appears as the most active (i.e. $T_{95\%}$ = 356 °C), overcoming the pure ceria performance (Fig. 8B) probably associated with the improvement in oxygen mobility due to the insertion of Zr into the ceria lattice detected at 450 °C (see XRD analysis).

3.4. Reaction performance of catalytic membranes in n-C_6 combustion

The reaction performance of the Ce-Zr and Ce-Mn based catalytic membranes tested in *n*-hexane combustion is summarized in Table 3. The most striking effect is the activity enhancement exhibited by catalytic membranes prepared using 30 min as intermediate drying period (denoted with "*") provoked by the improvement in the catalyst confinement as is explained in Section 3.2. The $T_{95\%}$ values reported for MB/C*, MB/Z* and MB/M* compared with MB/C, MB/Z and MB/M dropped in 13, 71 and 42 °C, respectively.

Table 3
Performance of Ce-Zr and Ce-Mn based catalytic membranes in *n*-hexane combustion at reference conditions

Membrane	Total catalyst[a] loading (mg)	$T_{50\%}$ (°C)	$T_{95\%}$ (°C)
MB/C	38	344	436
MB/Z	18	340	466
MB/M	21	295	368
MB/C[a]	25	325	423
MB/Z[a]	24	308	395
MB/M[a]	8	249	326
MB/CZ[a]	31	309	405
MB/CM[a]	16	286	396

[a] Calculated by weight difference.

The most active catalytic membrane among simple oxide based samples is the corresponding to manganese oxide (MB/M*), followed by ZrO_2 (MB/Z*) and finally CeO_2 (MB/C*); in contrast with the results obtained for bulk samples, in which powdered ceria overcame the zirconia performance. However, MB/M* membrane is, by far, the unique sample (among the tested) which undergoes a strong deactivation with time on stream, even more pronounced than its bulk counterpart (the conversion becomes negligible after 12 h exposed at $T_{50\%}$ reaction conditions). Moreover, MB/C* membrane shows a negligible CO production whatever the conversion level achieved. Therefore, among single oxides based membranes, the pure ceria membrane could be considered as the most favourable sample in terms of activity, stability and selectivity to total combustion products.

Considering the Ce-Mn catalytic system, MB/CM* sample describes an intermediate performance between those corresponding to pure simple oxide membranes. According to SEM–EDX analysis (see Section 3.2), MB/CM* sample presents an average Ce/Mn atomic ratio around 1.5 within the top layer, although does not overcome the catalytic activity of pure single oxides in contrast with the observed behaviour for powdered samples with similar nominal composition (i.e. $Ce_{0.5}Mn_{0.5}O_2$ and $Ce_{0.67}Mn_{0.33}O_2$ samples). However, no deactivation phenomenon has been observed for Ce-Mn based catalytic membranes tested at reference conditions. The thermal stability achieved in these samples suggests that the porous support is a quite well dispersion framework thanks to which Ce-Mn oxides are suitably dispersed to stabilize the system.

Considering Ce-Zr series, the light-off curves obtained for MB/C*, MB/Z* and MB/CZ* nearly overlap each other (i.e. $T_{50\%}$ and $T_{95\%}$ values are rather close), a more pronounced trend than the observed for the homologue bulk series. It is worthwhile to emphasize that the average Ce/Zr atomic ratio within the top layer for MB/CZ* differs substantially to the

bulk catalyst formulation (from 0.44 to 3.5 for membrane and powder, respectively).

Among the tested catalytic membranes, MB/CM* sample could be considered the most favourable candidate in terms of activity, selectivity and thermal stability at reaction conditions. However, the catalyst distribution might be greatly improved according to SEM-EDX observations, fully detailed in Section 3.2, because a substantial part of the catalyst is not located within the mesoporous top layer where the gas–solid contact is maximized. Therefore, both fixed bed and membrane reactor configurations are compared at different 'effective' weight hourly space velocity values, always in detrimental for catalytic membrane reactors (i.e. $T_{50\%}$ values of 269 and 325 °C for CeO_2 and MB/C*, respectively).

4. Conclusions

In this work, cerium based oxides in powder form have been prepared by coprecipitation followed by calcination at moderate temperatures (350 or 450 °C) in order to preserve catalyst surface area. No XRD peaks or TPR signals attributed to single oxides have been observed for mixed samples. In general, mixed oxides exhibit a face centered cubic cell typical of the fluorite structure. For Ce-Mn series, a systematic peak width broadening was observed with increasing manganese content, indicating the occurrence of more defective cerianite lattice and lower degree of crystallinity in agreement with the BET surface area measurements. Moreover, the BET area values of all the composites outweighed that predicted for mere mechanical mixtures of pure Mn_xO_y and CeO_2 as a result of the intimate interaction between both oxides, also demonstrated by TPR and XPS analysis. Particularly, Ce-Mn oxides with a Mn atomic percentage greater than 50% show the best catalytic performance in *n*-hexane combustion at ppm level, outperforming the activity of pure single oxides. Reducibility of the mixed oxide, associated with the presence of more manganese oxide species in higher oxidation states, has been revealed as the key parameter controlling the catalytic activity. In such a way, Ce-Mn oxides synthesised by the alternative method (denoted as B), which results in a smaller Mn^{4+} content, are less active than those prepared by the conventional standard route in spite of the higher surface area developed by the former ones.

Unlike Ce-Mn series, Ce-Zr oxides calcined at 350 °C does not overcome the catalytic activity of pure single oxides. On the other hand, $Ce_{0.78}Zr_{0.22}O_2$h sample exhibits a light-off temperature value lower than those registered for pure CeO_2 and ZrO_2 solids, indicating that surface area alone cannot account for the reaction performance achieved. In addition, the XRD data processing carried out over the Ce-Zr series calcined at 450 °C reveals that for the mixed composition the insertion of zirconium into the ceria lattice has been accomplished explaining the improved catalytic performance.

Although Ce-Mn powdered catalysts appear more active in *n*-hexane combustion than their Ce-Zr counterparts; a strong deactivation phenomenon, more severe for Mn rich samples, is observed with time on stream in contrast with Ce-Zr based samples showing catalytic stability under equivalent reaction conditions.

The developed preparation procedure of analogous catalytic membranes has allowed us to preserve the Knudsen diffusion permeation pattern distinctive of the asymmetric structure of the starting alumina supports. The Ce-metal atomic ratio within the top layer evaluated by SEM-EDX analysis differs from the nominal value and is always higher for Ce-Mn based membranes. When the metal chemical environments of bulk and supported mixed samples are compared is observed that manganese and zirconium oxidation states of surface species are rather similar.

From preliminary preparation tests carried out with shorter membranes, it can be concluded that the concentration of precursor solution, the intermediate drying period and the reagent–contact configuration are clearly affecting the catalyst loading and distribution inside the membrane thickness. A short intermediate drying period is favourable in order to obtain a better catalyst confinement inside the mesoporous layer of γ-Al_2O_3 membrane enhancing the catalytic performance. Under equivalent conditions, the confinement is more easily achievable for the Ce-Mn system than for the Ce-Zr counterpart, and improves with the concentration of the mixed starting precursor.

Among single oxides based membranes, the pure ceria membrane could be considered as the most favourable sample in terms of activity, stability and selectivity to total combustion products. Nevertheless, the catalytic membrane reactor results reveal that solid distribution could be greatly improved due to a substantial part of the catalyst is not participating in the reaction. This fact would allow us to explain the reactor performance differences observed when fixed bed and catalytic membrane configurations are compared whatever the catalyst composition. Therefore, a suitable deposition of mixed oxide material remains a task to overcome in the near future, in particular for the Ce-Zr system. Finally, it is worthwhile to remark the thermal stability exhibited by the Ce-Mn catalytic membranes in contrast with the corresponding bulk catalysts behaviour. This result supposes a promising advantage of the γ-Al_2O_3 membrane based reactor in order to achieve a stable operation in the catalytic abatement of volatile organic compounds.

References

[1] Directive 2000/69/EC of the European Parliament and of the Council of 16 November 2000 relating to limit values for benzene and carbon monoxide in ambient air, Official J. Euro. Commun. L313/12. 13 December 2000.
[2] J.J. Spivey, Complete catalytic oxidation of volatile organics, Ind. Eng. Chem. Res. 26 (1987) 2165–2180.
[3] A. Gil, M.A. Vicente, J.F. Lambert, L.M. Gandía, Platinum catalysts supported on Al-pillared clays: application to the catalytic combustion of acetone and methyl-ethyl-ketone, Catal. Today 68 (2001) 41–51.
[4] S. Ordóñez, L. Bello, H. Sastre, R. Rosal, F.V. Díez, Kinetics of the deep oxidation of benzene, toluene, *n*-hexane and their binary mixtures over a platinum on γ-alumina catalyst, Appl. Catal. B: Environ. 38 (2002) 139–149.
[5] S. Scirè, S. Minicò, C. Crisafulli, Pt catalysts supported on H-type zeolites for the catalytic combustion of chlorobenzene, Appl. Catal. B: Environ. 45 (2003) 117–125.
[6] K. Okumura, T. Kobayashi, H. Tanaka, M. Niwa, Toluene combustion over palladium supported on various metal oxide supports, Appl. Catal. B: Environ. 44 (2003) 325–331.

[7] M.A. Centeno, M. Paulis, M. Montes, J.A. Odriozola, Catalytic combustion of volatile organic compounds on $Au/CeO_2/Al_2O_3$ and Au/Al_2O_3 catalysts, Appl. Catal. A: Gen. 234 (2002) 65–78.
[8] S. Scirè, S. Minicò, C. Crisafulli, C. Satriano, A. Pistone, Catalytic combustion of volatile organic compounds on gold/cerium oxide catalysts, Appl. Catal. B: Environ. 40 (2003) 43–49.
[9] H. Rotter, M.V. Landau, M. Carrera, D. Goldfarb, M. Herskowitz, High surface area chromia aerogel efficient catalyst and catalyst support for ethylacetate combustion, Appl. Catal. B: Environ. 47 (2004) 111–126.
[10] C. Mazzocchia, A. Kaddouri, On the activity of copper chromite catalysts in ethyl acetate combustion in the presence and absence of oxygen, J. Mol. Catal. A: Chem. 204–205 (2003) 647–654.
[11] A. Trovarelli, M. Boaro, E. Rocchini, C. De Leitenburg, G. Dolcetti, Some recent developments in the characterization of ceria-based catalysts, J. Alloys Compd. 323 (2001) 584–591.
[12] D. Terribile, A. Trovarelli, C. De Leitenburg, A. Primavera, G. Dolcetti, Catalytic combustion of hydrocarbons with Mn and Cu-doped ceria–zirconia solid solutions, Catal. Today 47 (1999) 133–140.
[13] A. Trovarelli, C. De Leitenburg, M. Boaro, G. Dolcetti, The utilization of ceria in industrial catalysis, Catal. Today 50 (1999) 353–367.
[14] C.E. Hori, H. Permana, K.Y. Simon, A. Brenner, K. More, K.M. Rahmoeller, D. Belton, Thermal stability of oxygen storage properties in a mixed CeO_2-ZrO_2 system, Appl. Catal. B: Environ. 16 (1998) 105–117.
[15] C.E. Hori, A. Brenner, K.Y. Simon, K.M. Rahmoeller, D. Belton, Studies of the oxygen release in the platinum-ceria-zirconia system, Catal. Today 50 (1999) 299–308.
[16] S. Rossignol, Y. Madier, D. Duprez, Preparation of zirconia-ceria materials by soft-chemistry, Catal. Today 50 (1999) 261–270.
[17] S. Letichevsky, C.A. Tellez, R.R. De Avillez, M.I. Da Silva, M.A. Fraga, L.G. Appel, Obtaining CeO_2-ZrO_2 mixed oxides by coprecipitation: role of preparation conditions, Appl. Catal. B: Environ. 58 (2005) 203–210.
[18] P. Ciambelli, S. Cimino, S. De Rossi, M. Faticanti, L. Lisi, G. Minelli, I. Pettiti, P. Porta, G. Russo, M. Turco, $AMnO_3$ (A = La, Nd, Sm) and $Sm_{1-x}Sr_xMnO_3$ perovskites as combustion catalysts: structural, redox and catalytic properties, Appl. Catal. B: Environ. 24 (2000) 243–253.
[19] R. Spinicci, A. Tofanari, M. Faticanti, I. Pettiti, P. Porta, Hexane total oxidation on $LaMO_3$ (M = Mn, Co, Fe) perovskite-type oxides, J. Mol. Catal. A: Chem. 176 (2001) 247–252.
[20] I. Barrio, I. Legorburu, M. Montes, M.I. Domínguez, M.A. Centeno, J.A. Odriozola, New redox deposition-precipitation method for preparation of supported manganese oxide catalysts, Catal. Lett. 101 (3–4) (2005) 151–157.
[21] L.M. Gandía, A. Gil, S.A. Korili, Effects of various alkali–acid additives on the activity of a manganese oxide in the catalytic combustion of ketones, Appl. Catal. B: Environ. 33 (2001) 1–8.
[22] J. Villaseñor, P. Reyes, G. Pecchi, Catalytic and photocatalytic ozonation of phenol on MnO_2 supported catalysts, Catal. Today 76 (2002) 121–131.
[23] M. Baldi, E. Finocchio, F. Milella, G. Busca, Catalytic combustion of C3 hydrocarbons and oxygenates over Mn_3O_4, Appl. Catal. B: Environ. 16 (1998) 43–51.
[24] S. Imamura, M. Shono, N. Okamoto, A. Hamada, S. Ishida, Effect of cerium on the mobility of oxygen on manganese oxides, Appl. Catal. A: Gen. 142 (1996) 279–288.
[25] A. Keshavaraja, A.V. Ramaswamy, Mn-stabilized zirconia catalysts for complete oxidation of *n*-butane, Appl. Catal B: Environ. 8 (1996) L1–L7.
[26] C. De Leitenburg, D. Goi, A. Primavera, A. Trovarelli, G. Dolcetti, Wet oxidation of acetic acid catalysed by doped ceria, Appl. Catal. B: Environ. 11 (1996) L29–L35.
[27] G. Blanco, M.A. Cauqui, J.J. Delgado, A. Galtayries, J.A. Perez-Omil, J.M. Rodríguez-Izquierdo, Preparation and characterization of Ce-Mn-O composites with applications in catalytic wet oxidation processes, Surf. Interface Anal. 36 (8) (2004) 752–755.
[28] S. Imamura, K. Doi, S. Ishida, Wet oxidation of ammonia catalyzed by cerium-based composite oxides, Ind. Eng. Chem. Prod. Res. Dev. 24 (1985) 75–80.
[29] S. Imamura, M. Nakamura, N. Kawabata, J. Yoshida, S. Ishida, Wet oxidation of Poly(ethylene glycol) catalyzed by manganese-cerium composite oxide, Ind. Eng. Chem. Prod. Res. Dev. 25 (1986) 34–37.
[30] H. Chen, A. Sayari, A. Adnot, F. Larachi, Composition-activity effects of Mn-Ce-O composites on phenol catalytic wet oxidation, Appl. Catal. B: Environ. 32 (2001) 195–204.
[31] E. Díaz, S. Ordoñez, A. Vega, J. Coca, Catalytic combustion of hexane over transition metal modified zeolites NaX and CaA, Appl. Catal. B: Environ. 56 (2005) 313–322.
[32] A. Julbe, D. Farruseng, C. Guizard, Porous ceramic membranes for catalytic reactors: overview and new ideas, J. Membr. Sci. 181 (1) (2001) 3–20.
[33] M.P. Pina, M. Menéndez, J. Santamaria, The Knudsen-diffusion catalytic membrane reactor: an efficient contactor for the combustion of volatile organic compounds, Appl. Catal. B: Environ. 11 (1) (1996) L19–L27.
[34] M.P. Pina, S. Irusta, M. Menéndez, J. Santamaría, R. Hughes, N. Boag, Combustion of volatile organic compounds over Pt-based catalytic membrane reactors, Ind. Eng. Chem. Res. 36 (1997) 4557–4566.
[35] S. Zalamea, M.P. Pina, A. Villellas, M. Menéndez, J. Santamaría, Combustion of volatile organic compounds over mixed-regime catalytic membranes, React. Kinet. Catal. Lett. 67 (1) (1999) 13–19.
[36] S. Irusta, M.P. Pina, M. Menéndez, J. Santamaría, Development and application of perovskite-based catalytic membrane reactors, Catal. Lett. 54 (1998) 69–78.
[37] G. Picasso, A. Quintilla, M.P. Pina, J. Herguido, Total combustion of methyl-ethyl ketone over Fe_2O_3 based catalytic membrane reactors, Appl. Catal. B: Environ. 46 (2003) 133–143.
[38] K. Keizer, R.J.R. Ulhorn, R.J. Van Vuren, A.J. Burgraaf, Gas separation mechanisms in microporous modified γ-Al_2O_3 membranes, J. Membr. Sci. 39 (1988) 285–300.
[39] M.H. Yao, R.J. Baird, F.W. Kunz, T.E. Hoost, An XRD investigation of the structure of alumina-supported ceria-zirconia, J. Catal. 166 (1997) 67–74.
[40] C. Bozo, N. Guilhaume, E. Garbowski, M. Primet, Combustion of methane on CeO_2-ZrO_2 based catalysts, Catal. Today 59 (2000) 33–45.
[41] A. Gil, L.M. Gandía, S.A. Korili, Effects of the temperature of calcinations on the catalytic performance of manganese and samarium-manganese-based oxides in the complete oxidation of acetone, Appl. Catal. A: Gen. 274 (2004) 229–235.
[42] X. Tang, Y. Li, X. Huang, Y. Xu, H. Zhu, J. Wang, W. Chen, MnO_x-CeO_2 mixed oxide catalysts for complete oxidation of formaldehyde: effect of preparation method and calcination temperature, Appl. Catal. B: Environ. 62 (2006) 265–273.
[43] F. Larachi, J. Pierre, Adnot, A. Bernis, Ce 3d XPS study of composite $Ce_xMn_{1-x}O_{2-y}$ wet oxidation catalysts., Appl. Surf. Sci. 195 (2002) 236–250.
[44] G. Picasso, Doctoral Thesis in "Combustión de COVs mediante Reactores de Membrana Catalítica Mesoporosa basadas en Oxidos Metálicos. Estudio cinético y Simulación", 2005.